The Role of the Ethynyl Substituent on the π–π Stacking Affinity of Benzene: A Theoretical Study

ARTICLE *in* CHEMPHYSCHEM · FEBRUARY 2011

Impact Factor: 3.42 · DOI: 10.1002/cphc.201000891 · Source: PubMed

4 AUTHORS:

Xavier Lucas
University of Dundee
18 PUBLICATIONS **171** CITATIONS
SEE PROFILE

David Quiñonero
University of the Balearic Islands
139 PUBLICATIONS **4,159** CITATIONS
SEE PROFILE

Antonio Frontera
University of the Balearic Islands
276 PUBLICATIONS **5,606** CITATIONS
SEE PROFILE

Pere M Deyà
University of the Balearic Islands
172 PUBLICATIONS **4,671** CITATIONS
SEE PROFILE

DOI: 10.1002/cphc.201000891

The Role of the Ethynyl Substituent on the π–π Stacking Affinity of Benzene: A Theoretical Study

Xavier Lucas,* David Quiñonero, Antonio Frontera,* and Pere M. Deyà[a]

Herein, we report a high-level theoretical study (SCS-RI-MP2-(full)/aug-cc-pVTZ) examining the stacking affinity of 1,3,5-triethynylbenzene. The stacking properties of this compound are compared to those of benzene and 1,3,5-trifluorobenzene. The results indicate that the ethynyl substituent improves the stacking affinity of the arene, since the binding energies for the stacked ethynyl-substituted arene dimers are higher than those of both benzene and the fluoro-substituted arene. This interesting behaviour has been studied by examining the energetics, geometries and electron charge density features of the complexes. A query in the Cambridge Structural Database returned several X-ray crystal structures containing π–π stacking interactions of 1,3,5-triethynylaryls that strongly agree with the theoretical results.

1. Introduction

A spectacular development of supramolecular chemistry has been observed in terms of potential applications and in its relevance to analogous biological systems. A great variety of noncovalent forces regulate the formation and function of supramolecular complexes. It is crucial to understand and quantify these intermolecular interactions in order to succeed in the rational design of new supramolecular systems, including intelligent materials, as well as for developing new biologically active agents.[1] In particular, interactions involving aromatic rings are very important in supramolecular chemistry.[2] Aromatic rings can participate in several noncovalent interactions either by the π-cloud (C–H/π,[3] cation–π,[4] anion–π,[5] lp/π[6]) or using the hydrogen atoms to participate in unconventional hydrogen bonds. In the case of heteroaromatic rings, strong hydrogen bonds can be established with hydrogen bond donors.

The π-basicity/acidity of aromatic rings can be modulated using substituents. The π-cloud of the benzene is affected by the substitution, thus making it possible to turn the ring into electron-poor or electron-rich by substituting hydrogen atoms by electron-withdrawing groups or electron donor groups, respectively. Our group has recently reported a high-level theoretical study analyzing the dual effect of the ethynyl group on the ion–π binding affinity of the benzene ring.[7] In that study we demonstrated that the anion–π complexes of 1,3,5-triethynylbenzene are energetically more favourable than those of benzene, whereas the interaction energies of the cation–π complexes are almost unaffected when compared to benzene. A deep analysis of the implications of the ethynyl substitution in benzene rings also showed that the introduction of ethynyl chains adds the ability to finely tune the ion–π affinity of electron-withdrawing- and electron-donor-substituted arenes with anions and cations, respectively.[8] Herein our group focuses its attention on the π–π stacking affinity of 1,3,5-triethynylbenzene, as the understanding of its π-binding abilities is of crucial interest to rationalize recent developments in material science and crystal engineering.[9] We report herein a high-level ab initio study where we analyse the role of the ethynyl group as a substituent in the face-to-face and parallel-displaced stacking interactions of benzene. We computed the compounds and complexes shown in Figure 1 and analysed their physico-chemical properties. Moreover, we used Bader's theory of atoms in molecules (AIM)[10] to describe the interactions. The theoretical study gives interesting clues on the stacking affinity of 1,3,5-triethynylbenzene, since all its complexes have higher binding

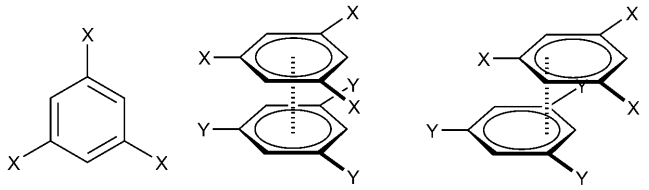

1, X = H
2, X = F
3, X = CCH

4, X = Y = H
5, X = F, Y = H
6E, X = Y = F
6A, X = Y = F
7, X = CCH, Y = H
8E, X = Y = CCH
8A, X = Y = CCH

9, X = Y = H
10E, X = F, Y = H
10A, X = F, Y = H
11E, X = Y = F
11A, X = Y = F
12E, X = CCH, Y = H
12A, X = CCH, Y = H
13E, X = Y = CCH
13A, X = Y = CCH

Figure 1. Compounds **1**–**3** and complexes **4**–**13** studied herein. **E** and **A** refer to the eclipsed and alternated conformations, respectively.

[a] *X. Lucas, Dr. D. Quiñonero, Dr. A. Frontera, Prof. Dr. P. M. Deyà*
Department of Chemistry
Universitat de les Illes Balears
Crta. de Valldemossa km 7.5, 07122 Palma de Mallorca (Spain)
Fax: (+34) 971173426
E-mail: xlc1986@gmail.com
toni.frontera@uib.es

Supporting information for this article is available on the WWW under http://dx.doi.org/10.1002/cphc.201000891.

energies than those obtained for either benzene or 1,3,5-trifluorobenzene. The theoretical prediction indicates that the preferred conformation is the alternated parallel-displaced stacking, while both the alternated face-to-face and the eclipsed parallel-displaced stacking orientations have similar but also high affinity. The eclipsed face-to-face stacking remains as the poorest alternative. In order to compare our theoretical results with experimental data, we performed a systematic search in the Cambridge Structural Database (CSD) to find evidence of complexes that present π–π stacking interactions of 1,3,5-triethynylaryls. The exploration of the CSD returns 19 X-ray structures of crystals that fulfill our request. Most of them belong to parallel-displaced conformations.

2. Results and Discussion

The aim of this study is to analyse the effect of the substitution of hydrogen atoms with ethynyl groups on the stacking ability of benzene, since we have found striking and unexpected ion–π properties of 1,3,5-triethynylbenzene (Lucas et al.[7,8]). To this end, we gather in Table 1 the energetics, geometries and electron densities obtained for the complexes **4**–**13** (see Figure 1). The values for the electron charge density (ρ) are obtained performing a topological analysis and studying the distribution and properties of the critical points (CP) applying Bader's AIM theory to the MP2(full)/aug-cc-pVDZ//SCS-RI-MP2(full)/aug-cc-pVTZ wavefunction. For the face-to-face stacked complexes **4**–**8**, exploration of the CPs revealed the presence of several bond (BCP) and ring (RCP) critical points (see Table 1), but a unique cage CP (CCP) placed at the center of the stacking interaction along the main symmetry axis. For that reason, the electron density at the CCP is given as the electron density descriptor of the interaction. For the parallel-displaced complexes **9**–**13** a more complicated situation arises: several BCPs, RCPs and CCPs appear for the complexes. For the sake of coherence, we selected the CCP with the highest electron density value, which is given in Table 1. The value of the electron charge density (ρ) computed at the cage CP in π–π complexes has been related to the strength of the interaction and thus can be used as a measure of the bond order.[11]

Table 1. Binding energies with BSSE correction, E_{BSSE} [kcal mol^{-1}], and equilibrium centroid-to-centroid distances, R [Å], at the SCS-RI-MP2(full)/aug-cc-pVTZ level of theory for complexes **4**–**13**. Distribution of critical points (B, R and C indicate the number of bond, ring and cage CPs, respectively) and electron charge density at the (3,+3) critical point, ρ [a.u.], at the MP2(full)/aug-cc-pVDZ level of theory. Symmetry imposed during the optimization is also given.

Compound	X	Y	E_{BSSE}	R[a]	$10^3\rho$	B, R, C	Sym
4	H	H	−1.6	3.69	1.6	6, 6, 1	D_{2h}
5	F	H	−2.9	3.49	2.2	3, 3, 1	C_s
6E	F	F	−2.4	3.47	2.3	3, 3, 1	C_{2v}
6A	F	F	−3.4	3.34	2.8	6, 6, 1	C_{2h}
7	CCH	H	−4.0	3.42	2.2	6, 6, 1	C_s
8E	CCH	CCH	−4.3	3.49	2.0	9, 9, 1	C_{2v}
8A	CCH	CCH	−6.8	3.25	2.8	6, 6, 1	C_{2h}
9	H	H	−2.3	3.68 (3.28)	3.9	2, 3, 2	C_{2h}
10E	F	H	−3.2	3.51 (3.29)	4.5	4, 5, 2	C_s
10A	F	H	−4.1	3.52 (3.19)	5.3	3, 4, 2	C_s
11E	F	F	−3.2	3.46 (3.18)	5.2	4, 6, 3	C_s
11A	F	F	−3.8	3.39 (3.14)	5.8	2, 3, 2	C_{2h}
12E	CCH	H	−4.6	3.46 (3.27)	4.4	4, 5, 2	C_s
12A	CCH	H	−5.6	3.47 (3.19)	5.1	3, 4, 2	C_s
13E	CCH	CCH	−6.8	3.58 (3.16)	4.6	5, 6, 2	C_s
13A	CCH	CCH	−7.6	3.30 (3.09)	6.0	4, 5, 2	C_{2h}

[a] Values in parenthesis correspond to centroid-to-plane equilibrium mean distances [Å].

A general view of the results gathered in Table 1 shows negative interaction energies (E_{BSSE}) for all complexes, indicating a favourable interaction between the different pairs of monomers. The interaction energies for the face-to-face stacked complexes **4**–**8** are less favourable than those of the corresponding parallel-displaced complexes **9**–**13**. Moreover, the electronic repulsion between the substituents provokes the interaction energies for the alternated conformations to be more negative than those of the corresponding eclipsed conformations. Since we are interested in the effect of the substitution on the stacking ability of arenes, we have divided our analysis according to the two types of stacking interactions studied herein.

2.1. Face-to-Face Stacked Complexes 4–8

The interaction energy of the benzene dimer **4** is −1.6 kcal mol^{-1} (Table 1) in agreement with calculations at higher levels of theory.[12] The substitution of hydrogen atoms by fluorine atoms at one of the benzene monomers leads to the formation of the heterodimeric fluoro-substituted complex **5**. This process implies an increase of the interaction energy of −1.3 kcal mol^{-1}, in line with the increase in the π-acidity of the substituted arene. Substitution at the second benzene ring leads to the formation of the corresponding eclipsed and alternated homodimeric complexes **6E** and **6A**. The interaction energy of **6A** is −3.4 kcal mol^{-1}, indicating a strengthening of the interaction when compared either to the homodimeric benzene complex **4** or the heterodimeric complex **5** (their interaction energies are −1.6 and −2.9 kcal mol^{-1}, respectively). The interaction energy for **6E** (−2.4 kcal mol^{-1}) is less favourable than that of **5**, indicating that the substitution at the second benzene provokes a weakening of the stacking interaction. For the ethynyl-substituted arenes, the formation of the heterodimeric complex **7** implies an increase of the interaction energy of 2.4 kcal mol^{-1} when compared to the benzene dimer **4** (the interaction energies are −4.0 and −1.6 kcal mol^{-1}, respectively). With substitution at the second monomer the interaction energies of both the homodimeric ethynyl-substituted eclipsed and alternated compounds **8E** and **8A** are more favourable than **7** (−0.3 and −2.8 kcal mol^{-1}, respectively), in contrast to the fluoro-substituted arenes. It is interesting to point out the interaction energy observed for the complex **8A** of −6.8 kcal mol^{-1}, which actually doubles the interaction energy of its fluoro-substituted homologue **6A**, −3.4 kcal mol^{-1}. Also the theoretical rotation from the eclipsed homodimeric ethynyl-substituted arene **8E** to the alternated

complex **8A** represents a gain in interaction energy of 2.5 kcal mol^{-1}, in contrast to the gain of 1.0 kcal mol^{-1} observed for the fluorine complexes **6E** to **6A**. In Figure 2 we show the molecular electrostatic potential (MEP) representation for 1,3,5-triethynylbenzene **3**, in order to shed light from an electrostatic point of view on the higher affinity of this compound to adopt the alternated stacking conformation in the dimer. In this conformation, regions with negative electrostatic potential (near the C≡C bonds, in red) face regions with positive electrostatic potential (benzene hydrogen atoms, in green) and vice versa. This phenomenon increases the electrostatic attraction of the monomers and literally "traps" them in the dimeric complex.

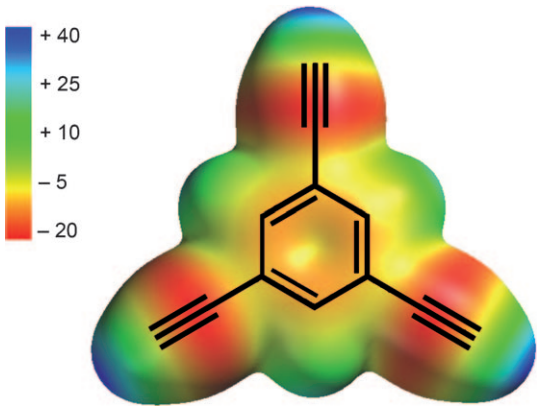

Figure 2. MEP representation for 1,3,5-triethynylbenzene **3**. The potential energy is given in kcal mol^{-1}.

The geometry parameters are also gathered in Table 1. The equilibrium distances of the optimized complexes can be related to the strength of the interaction. Shorter distances are indicative of stronger interactions and vice versa. The substituted face-to-face stacked compounds **5**–**8** have shorter equilibrium distances than the benzene–benzene dimer **4** in agreement with the energetic results and the strengthening of the π–π interaction. The shortening of the equilibrium distances is more evident in the alternated dimers, reaching 0.35 Å for the fluoro-substituted arene **6A** and 0.44 Å for the ethynyl-substituted complex **8A**. The electron charge density values at the CCP (ρ) are also included in Table 1. Large values of ρ are related to stronger interactions and vice versa. In agreement with the energetics and geometries, ρ has its minimum for the benzene homodimer and its maximum for the alternated face-to-face stacked complexes **6A** and **8A**. We show in Figure 3 (top) the distribution of CPs and pathways obtained for the latter compound. The pathways show that the arenes interact through six BCPs that link their carbon atoms, six RCPs and one central CCP that is connected to six RCPs that characterize the π–π interaction and to the aromatic RCPs.

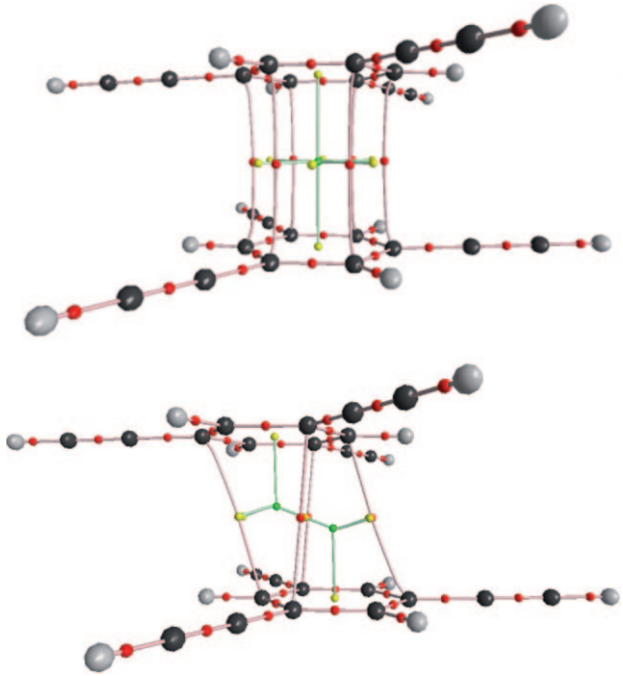

Figure 3. Distribution of critical points (bond in red, ring in yellow and cage in green) and pathways (bond in red and cage in green) for 1,3,5-triethynylbenzene dimers in the face-to-face **8A** (top) and parallel-displaced **13A** (bottom) complexes. The pathways connecting (3,-3) and (3,-1) CPs are shown in pink and pathways connecting (3,+1) and (3,+3) CPs are shown in green.

2.2. Parallel-Displaced Stacked Complexes 9–13

The interaction energy of the parallel-displaced stacked benzene dimer **9** is −2.3 kcal mol^{-1} (see Table 1), in agreement with the higher-level results available in the literature.[12] When one benzene ring is exchanged by a 1,3,5-trifluorobenzene ring two possible conformations can be adopted. One conformation is the eclipsed heterodimer **10E**, where one fluorine is located over the benzene ring. The other conformation is the alternated complex **10A**, where a hydrogen atom instead of a fluorine atom is located over the benzene ring (see Figures 1 and 4). These substitutions cause an increase in interaction energy for both the eclipsed and alternated conformations of 0.9 and 1.8 kcal mol^{-1}, respectively. When the second benzene is substituted an interesting point arises, because none of the stacking conformations is strengthened. Curiously, the eclipsed homodimer **11E** and heterodimer **10E** present the same inter-

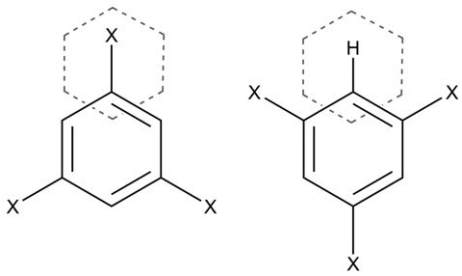

Figure 4. Schematic top-view representation of the heterodimeric parallel-displaced complexes studied herein. For the eclipsed dimers (**10E** and **12E**) the substituent is located over the benzene ring (left) and for the alternated dimers (**10A** and **12A**) a hydrogen atom is located over the benzene ring (right).

action energy (-3.2 kcal mol^{-1}). For the alternated fluoro-substituted homodimeric complex **11A** the interaction energy is less favourable compared to the heterodimer **10A**, since the interaction energies are -3.8 and -4.1 kcal mol^{-1}, respectively, indicating that the interaction is weakened. Concerning the ethynyl-substituted series, the substitution of a benzene ring in the homodimeric complex **9** can also lead to two different parallel-displaced dimers. One conformation is the eclipsed heterodimer **12E**, where one ethynyl group is located over the benzene ring. The other conformation is the alternated complex **12A**, where a hydrogen atom instead of an ethynyl group is located over the benzene ring (see Figures 1 and 4). For **12E** and **12A** a strengthening of the interaction energies (2.3 kcal mol^{-1} and 3.3 kcal mol^{-1}, respectively) is observed compared to the benzene dimer **9**, indicating in both cases a strengthening of the stacking interaction. The interaction energies of the eclipsed **13E** and alternated **13A** homodimeric ethynyl-substituted complexes are -6.8 and -7.6 kcal mol^{-1}, respectively. These energies represent a reinforcement of the interaction of 4.5 kcal mol^{-1} and 5.3 kcal mol^{-1}, respectively, when compared to the benzene dimer **9** and a reinforcement of 2.2 kcal mol^{-1} and 2.0 kcal mol^{-1} when compared to the corresponding heterodimers **12E** and **12A**, respectively. It is worth noting that in both stacking conformations the interaction strengthens when the dimer is fully substituted, in contrast to the corresponding fluoro-substituted analogues **11E** and **11A**.

The geometry parameters for these complexes are also gathered in Table 1. The centroid-to-centroid equilibrium distance has its maximum for the benzene dimer **9**, in agreement with the energetic values. The shortening of both the centroid-to-centroid and the centroid-to-plane equilibrium distances is maximal for the homodimeric substituted complexes (0.29 and 0.14 Å, respectively, for the fluoro substitution in **11A**, and 0.39 and 0.19 Å, respectively, for the ethynyl-substituted complex **13A**). The electron charge density value at the CCP (ρ) has its minimum for the benzene dimer **9** and is maximal for the alternated ethynyl-substituted complex **13A**, in agreement with the energetics and geometry parameters. In Figure 3 (bottom) we included the distribution of CPs and pathways obtained for the latter. The aryls are connected through four BCPs, five RCPs and two CCPs connecting the rings and linked to each other by a central RCP.

2.3. Partitioning of the Energy

In Table 2 we summarize the DF-DFT-SAPT[13] energy values relative to the homodimeric benzenes (**4** and **9**) and ethynyl-substituted benzenes **8** and **13**. The SAPT interaction energies for these complexes are similar to those obtained using the SCS-RI-MP2(full)/aug-cc-pVTZ level of theory (see Table 1 and the energy plot in the Supporting Information, Figure S1). This similarity could be even better if the δ(HF) correction would have been calculated using a basis set larger than cc-pVDZ, which turned out to be computationally extremely expensive. It would be preferable to obtain the interaction energies by means of CCSD(T)/CBS calculations. However, these calculations are prohibitive due to the size of our systems. As expected for this type of interaction, the energy partitioning (Table 2) indicates that the dispersion term (E_{disp}) is the most important for the stability of the π–π stacking interactions, ranging from 13 to 19 kcal mol^{-1}. Moreover, the electrostatic term (E_{ee}) is of especially strong influence for the alternated face-to-face complex and both parallel-displaced complexes, reaching values that are higher than the interaction energy itself. For the eclipsed face-to-face complex, the small electrostatic term is in agreement with the MEP representation for this molecule (Figure 2), as regions with same electrostatic potential are facing each other. The exchange term (E_{exch}) counteracts part of these contributions, specially the dispersion term, increasing as the centroid-to-centroid or the centroid-to-plane distances decrease. Finally, the induction term (E_{ind}) has a very small value for all complexes. Therefore, it seems that the strengthened binding arises from the influence of E_{ee} together with a smaller influence of E_{disp}. The complete DF-DFT-SAPT results for all the homodimeric complexes studied herein are included in the Supporting Information (see Table S1).

Table 2. SAPT interaction energies and their partitioning into the electrostatic, induction, dispersion and exchange contributions (E_{SAPT}, E_{ee}, E_{ind}, E_{disp}, E_{exch}, respectively, [kcal mol^{-1}]) and the Hartree–Fock correction for higher-order contributions δ(HF) for the benzene dimers **4** and **9**, and for the homodimeric ethynyl-substituted benzenes **8** and **13** at the RI-DFT/aug-cc-pVTZ level of theory using the DF-DFT-SAPT approach.

Compound	E_{SAPT}	E_{ee}	E_{ind}	E_{disp}	E_{exch}	δ(HF)
4	−1.4	−0.5	−0.1	−6.0	5.4	−0.2
8E	−3.2	−2.2	−0.1	−12.9	12.3	−0.1
8A	−5.9	−7.0	−0.2	−16.0	18.0	−0.6
9	−2.2	−3.2	−0.2	−8.1	10.2	−0.8
13E	−5.4	−7.8	−0.3	−17.8	22.0	−1.5
13A	−5.8	−9.4	−0.4	−18.9	24.5	−1.7

2.4. CSD Results

We performed a systematic search in the Cambridge Structural Database in order to find evidences of crystal structures containing π–π stacking interactions of 1,3,5-triethynylaryls. We found 19 X-ray structures containing 30 π–π stacking interactions (see Table S2 in the Supporting Information for a complete list and crystallographic data). In Table 3 we classify these interactions and report geometry parameters and theoretical values for comparison. Most of the interactions are parallel-displaced (23 out of 30) or alternated face-to-face, in agreement with the energetic values. As expected, the crystallographic centroid-to-centroid distances are found to be larger than the equilibrium distances for the optimized geometries. The shortest distances correspond to the alternated face-to-face complexes, as predicted computationally (3.38 and 3.25 Å, respectively). In Figure 5 we schematically represent the computation of the displacement and rotational angles (β and α, respectively). β angles for the parallel-displaced interactions in the crystal are similar to those predicted theoretically, while the eclipsed dimers show a small rotation angle α between the rings, indi-

Table 3. Summary of crystal structures with intermolecular π–π stacking of 1,3,5-triethynylbenzene. **E** stands for the eclipsed and **A** for the alternated conformation. We included the number of interactions found, *n*, the centroid-to-centroid distance, *R* [Å], and the displacement and rotational angles, β and α [°], respectively. Binding energies, E_{BSSE} [kcal mol^{-1}], are also shown.

Compound	$n^{[a]}$	E_{BSSE}	$R^{[a,d]}$	$R^{[b]}$	$\beta^{[a,d]}$	$\beta^{[b]}$	$\alpha^{[a,d]}$	$\alpha^{[c]}$
8A	6	6.8	3.33–3.51 (3.38)	3.25	0.0–1.6 (0.4)	0.0	44–55 (47)	60
13E	11	6.8	3.60–4.22 (3.85)	3.58	9.5–35.0 (22.8)	28.1	0–14 (5)	0
13A	11	7.6	3.43–3.97 (3.67)	3.30	9.4–31.3 (19.8)	20.3	43–60 (53)	60

[a] Crystallographic values. [b] Predicted theoretical values. [c] Value imposed by symmetry restrictions. [d] Values are given as minimum–maximum (mean).

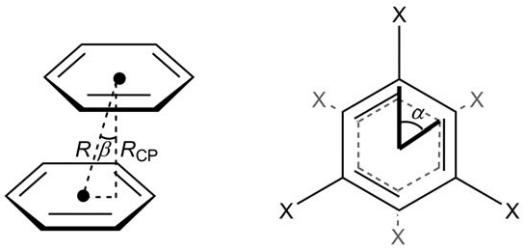

Figure 5. Schematic representation for the calculation of displacement and rotational angles (β and α, respectively) in the dimeric complexes studied. The centroid-to-centroid and centroid-to-plane distances are also shown (*R* and R_{CP}, respectively).

cating that the perfectly eclipsed conformation is not energetically favoured. As an example, in Figure 6 we show the crystal structures of alternated and eclipsed parallel-displaced π–π stacking interactions (CSD identifiers OCUKEC[14] and NIMREG,[15] respectively).

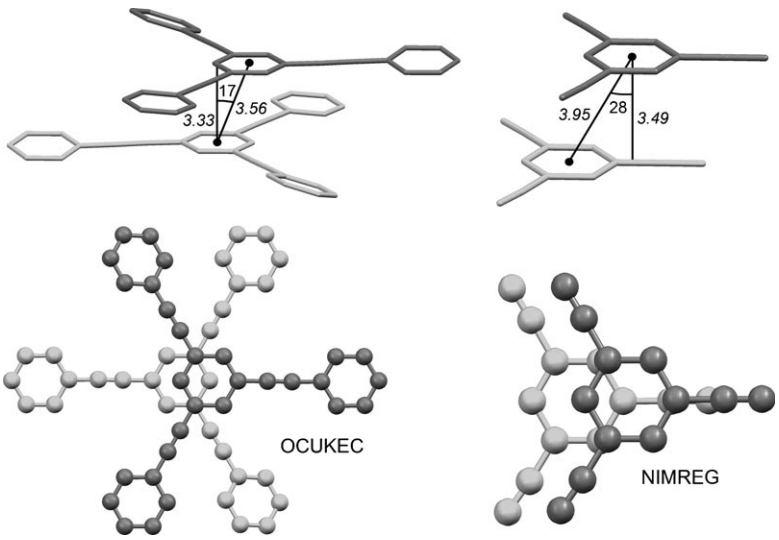

Figure 6. Perspective (top) and zenithal (bottom) views of two crystal structures containing parallel-displaced π–π stacking interactions of 1,3,5-triethynylaryls. Alternated (left, CSD identifier OCUKEC) and eclipsed (right, CSD identifier NIMREG) stacking arrangements are shown. We also included the displacement angles [°] as well as stacking and centroid-to-centroid distances [Å] (values in italics).

3. Conclusions

The results reported herein highlight the importance of the ethynyl substituent on the π–π stacking affinity of benzene dimers, as it has a strong influence on the interaction energy. It has been shown that the preferred conformation for the dimer corresponds to the alternated parallel-displaced stacking conformation. According to SAPT calculations this conformation is preferred due to electrostatic contributions and, to a lesser extend, to dispersion effects. A query in the CSD returned several crystal structures containing the different interactions studied herein. Since the interest for 1,3,5-triethynylaryls is growing rapidly in important fields like material science and supramolecular chemistry, a deep comprehension of their π properties is necessary.

Computational Methods

The geometries of the complexes studied in this report were fully optimized at the SCS-RI-MP2(full)/aug-cc-pVTZ level of theory with the program TURBOMOLE version 5.9.[16] The RI-MP2 method[17] previously applied for the study of cation–π and anion–π interactions is considerably faster than MP2 and the interaction energies and equilibrium distances are almost identical for both methods.[18] Moreover, we used the spin-component-scaled MP2 method (SCS-MP2), which is based on the scaling of the standard MP2 amplitudes for parallel and antiparallel spin double excitations.[19] The SCS-MP2 correlation treatment yields structures that are superior to those from standard MP2 calculations, particularly in systems that are dominated by dispersive interactions.[20] We computed the interaction energy for each complex by subtracting the total energy of the optimized monomers from the total energy of the complex in the optimized geometry. It was calculated at the same level of theory with correction for the basis set superposition error (E_{BSSE}) using the Boys–Bernardi counterpoise technique.[21] The optimizations of the molecular geometries were performed imposing the highest Abelian symmetry group for each case (see Table 1). Other possible conformations of the complexes were not considered because the ultimate aim of this study was to analyse the effect of the ethynyl substituent on the π–π binding properties of benzenes.

The atoms in molecules (AIM) analysis[22] was performed by means of the AIM2000 version 2.0 program[23] using the MP2(full)/aug-cc-pVDZ//SCS-RI-MP2(full)/aug-cc-pVTZ wavefunctions of the opti-

mized complexes. It should be mentioned that some criticism regarding the AIM theory has been recently published.[24] The disagreement basically arises from erroneously identifying the bond paths as chemical bonds.[25] The partitioning of the interaction energies into the individual electrostatic, induction, dispersion, and exchange-repulsion components was carried out performing density functional theory (DFT) combined with the symmetry-adapted perturbation theory (DFT-SAPT)[26] approach at the DF-DFT/aug-cc-pVTZ//SCS-RI-MP2(full)/aug-cc-pVTZ level of theory (see the Supporting Information for a more comprehensive treatment).

Acknowledgements

We thank the DGICYT of Spain (project CTQ2008-00841/BQU) for financial support. We thank the CESCA for computational facilities. D. Q. thanks the Ministerio de Ciencia e Innovación (MICINN) of Spain for a "Ramón y Cajal" contract.

Keywords: ab initio calculations · energy partitioning · host–guest systems · stacking interactions · supramolecular chemistry

[1] H.-J. Schneider, *Angew. Chem.* **2009**, *121*, 3982 – 4036; *Angew. Chem. Int. Ed.* **2009**, *48*, 3924 – 3977.
[2] E. A. Meyer, R. K. Castellano, F. Diederich, *Angew. Chem.* **2003**, *115*, 1244 – 1287; *Angew. Chem. Int. Ed.* **2003**, *42*, 1210 – 1250.
[3] M. Nishio, M. Hirota, Y. Umezawa, *The C–H/π Interaction. Evidence, Nature and Consequences*, Wiley-VCH, New York, **1998**.
[4] a) J. C. Ma, D. A. Dougherty, *Chem. Rev.* **1997**, *97*, 1303 – 1324; b) J. P. Gallivan, D. A. Dougherty, *Proc. Natl. Acad. Sci. USA* **1999**, *96*, 9459 – 9464; c) G. W. Gokel, S. L. D. Wall, E. S. Meadows, *Eur. J. Org. Chem.* **2000**, 2967 – 2978; d) G. W. Gokel, L. J. Barbour, S. L. D. Wall, E. S. Meadows, *Coord. Chem. Rev.* **2001**, *222*, 127 – 154; e) G. W. Gokel, L. J. Barbour, R. Ferdani, J. Hu, *Acc. Chem. Res.* **2002**, *35*, 878 – 886; f) C. A. Hunter, J. Singh, J. M. Thorton, *J. Mol. Biol.* **1991**, *218*, 837 – 846.
[5] a) M. Mascal, A. Armstrong, M. Bartberger, *J. Am. Chem. Soc.* **2002**, *124*, 6274 – 6276; b) I. Alkorta, I. Rozas, J. Elguero, *J. Am. Chem. Soc.* **2002**, *124*, 8593 – 8598; c) D. Quiñonero, C. Garau, C. Rotger, A. Frontera, P. Ballester, A. Costa, P. M. Deyà, *Angew. Chem.* **2002**, *114*, 3539 – 3542; *Angew. Chem. Int. Ed.* **2002**, *41*, 3389 – 3392.
[6] T. J. Mooibroek, P. Gamez, J. Reedijk, *CrystEngComm* **2008**, *10*, 1501 – 1515.
[7] X. Lucas, D. Quiñonero, A. Frontera, P. M. Deyà, *J. Phys. Chem. A* **2009**, *113*, 10367 – 10375.
[8] X. Lucas, A. Frontera, D. Quiñonero, P. M. Deyà, *J. Phys. Chem. A* **2010**, *114*, 1926 – 1930.
[9] a) S. Yuan, B. Dorney, D. White, S. Kirklin, P. Zapol, L. Yu, D. Liu, *Chem. Commun.* **2010**, *46*, 4547 – 4549; b) F. García, L. Sánchez, *Chem. Eur. J.* **2010**, *16*, 3138 – 3145; c) H. Yan, S. Lim, Y. Zhang, Q. Chen, D. Mott, W. Wu, D. An, S. Zhou, C. Zhong, *Chem. Commun.* **2010**, *46*, 2218 – 2220.
[10] R. F. W. Bader, *J. Phys. Chem. A* **1998**, *102*, 7314 – 7323.
[11] D. Quiñonero, A. Frontera, D. Escudero, P. Ballester, A. Costa, P. M. Deyà, *Theor. Chem. Acc.* **2008**, *120*, 385 – 393.
[12] R. Podeszwa, R. Bukowski, K. Szalewicz, *J. Phys. Chem. A* **2006**, *110*, 10345 – 10354.
[13] A. Heßelmann, G. Jansen, M. Schütz, *J. Chem. Phys.* **2005**, *122*, 014103.
[14] M. W. Day, A. J. Matzger, R. H. Grubbs, **2001**, private communication to the CSD, No. CCDC-130854.
[15] H. C. Weiss, D. Blaser, R. Boese, B. M. Doughan, M. M. Haley, *Chem. Commun.* **1997**, 1703 – 1704.
[16] R. Ahlrichs, M. Bär, M. Häser, H. Horn, C. Kömel, *Chem. Phys. Lett.* **1989**, *162*, 165 – 169.
[17] a) M. W. Feyereisen, G. Fitzgerald, A. Komornicki, *Chem. Phys. Lett.* **1993**, *208*, 359 – 363; b) O. Vahtras, J. Almlof, M. W. Feyereisen, *Chem. Phys. Lett.* **1993**, *213*, 514 – 518.
[18] a) D. Quiñonero, C. Garau, A. Frontera, P. Ballester, A. Costa, P. M. Deyà, *J. Phys. Chem. A* **2005**, *109*, 4632 – 4637; b) A. Frontera, D. Quiñonero, C. Garau, A. Costa, P. Ballester, P. M. Deyà, *J. Phys. Chem. A* **2006**, *110*, 5144 – 5148.
[19] a) S. Grimme, *J. Chem. Phys.* **2003**, *118*, 9095 – 9102; b) S. Grimme, *J. Comput. Chem.* **2003**, *24*, 1529 – 1537.
[20] M. Gerenkamp, S. Grimme, *Chem. Phys. Lett.* **2004**, *392*, 229 – 235.
[21] S. B. Boys, F. Bernardi, *Mol. Phys.* **1970**, *19*, 553 – 566.
[22] R. F. W. Bader, *Chem. Rev.* **1991**, *91*, 893 – 928.
[23] F. Biegler-König, J. Schönbohm, *J. Comput. Chem.* **2002**, *23*, 1489 – 1494.
[24] a) S. Grimme, C. Mück-Lichtenfeld, G. Erker, H. Wang, H. Beckers, H. Willner, *Angew. Chem.* **2009**, *121*, 2629 – 2633; *Angew. Chem. Int. Ed.* **2009**, *48*, 2592 – 2595; b) E. Cerpa, A. Krapp, A. Vela, G. Merino, *Chem. Eur. J.* **2008**, *14*, 10232 – 10234; c) E. Cerpa, A. Krapp, R. Flores-Moreno, K. J. Donald, G. Merino, *Chem. Eur. J.* **2009**, *15*, 1985 – 1990; d) J. Poater, M. Solà, F. M. Bickelhaupt, *Chem. Eur. J.* **2006**, *12*, 2902; e) A. Krapp, G. Frenking, *Chem. Eur. J.* **2007**, *13*, 8256 – 8270.
[25] R. F. W. Bader, *J. Phys. Chem. A* **2009**, *113*, 10391.
[26] a) A. Heßelmann, G. Jansen, *Chem. Phys. Lett.* **2002**, *362*, 319 – 325; b) A. Heßelmann, G. Jansen, *Chem. Phys. Lett.* **2002**, *357*, 464 – 470; c) A. Heßelmann, G. Jansen, *Chem. Phys. Lett.* **2003**, *367*, 778 – 784; d) A. Heßelmann, G. Jansen, *Phys. Chem. Chem. Phys.* **2003**, *5*, 5010 – 5014; e) G. Jansen, A. Heßelmann, *J. Phys. Chem. A* **2001**, *105*, 11156 – 11157.

Received: October 22, 2010
Revised: November 23, 2010
Published online on December 22, 2010

